NMR Study of the Drug–Base Overlap Geometry in the Dark Complex of 8-Methoxypsoralen and d(pApT)$_4$†

Roland Römer*,‡
Abteilung Biophysikalische Chemie, Zentrum Biochemie, Medizinische Hochschule, D-3000 Hannover, FRG
Angelika Anders
Institut für Biophysik, Universität Hannover, D-3000 Hannover, FRG
Received January 16, 1985

ABSTRACT: The dark binding of 8-methoxypsoralen (MOP) to d(pApT)$_4$ was investigated by 270-MHz ^{1}H nuclear magnetic resonance (NMR) spectra. The continuous high-field shifts of the MOP resonances by d(pApT)$_4$ at low temperatures indicate fast exchange between free and bound drug. The limiting complexation shifts of the various MOP protons between 0.36 (CH_3) and 1.20 ppm (H5) are in the range expected for an intercalation complex. The NMR line widths of the MOP ring protons vary with the square of the observed complexation shifts (maximum at H5), indicating a dominant effect of the fast exchange between free and bound drug. The corresponding kinetic parameters agree with the values previously reported for a variety of other intercalators. The observed exchange broadenings were also used as a criterion to limit the uncertainty connected with fast averaging of the signals of the drug in potential multiple binding modes: A qualitatively different pattern of broadenings (minimum at H5) is expected from fast exchange between the two binding modes related by the short 2-fold quasi-symmetry axis of MOP. The measured complexation shifts were compared to theoretical values calculated on the basis of coplanar intercalation with base pair arrangements derived from typical published intercalation site geometries. The standard deviation between observed and calculated shifts was considerably smaller for asymmetrical intercalation between the bases of the same strand ($\leq$0.11 ppm) than for symmetrical intercalation between the base pairs ($\geq$0.28 ppm). Our results indicate that in the equilibrium dark complex the base overlap geometry of MOP might not be favorable for the formation of the dominant *cis–syn*-furanoside photoadduct.

Psoralens, mainly 8-methoxypsoralen (MOP),[1] are applied for photosensitization in clinical photochemotherapy of skin diseases such as psoriasis and vitiligo (Parrish, 1981). In nucleic acid research, psoralens are used as molecular cross-linking probes for DNA and RNA. The photochemistry and photobiology of psoralens were reviewed by Song & Tapley (1979), Parsons (1980), and Hearst (1981).

The biological activities of psoralens are correlated with their photoreactivity toward DNA. Under UV irradiation, psoralens form two types of covalent photoproducts with DNA, mono-adducts and di-adducts, which cross-link the two strands of DNA. Thymine is the predominant base for the psoralen photocycloaddition to DNA, and the covalent bond is formed between its double bond and the 3,4 or 4′,5′ double bonds of the psoralen molecule. Recently, the cis–syn stereochemistry of the photoproducts of various psoralens and DNA has been reported (Kanne et al., 1982a,b; Peckler et al., 1982).

Intercalation of the drug between the DNA base pairs has been postulated as an important intermediate influencing the stereochemistry of the photochemical reactions (Cole, 1970; Dall'Acqua et al., 1971; Straub et al., 1981). Binding constants and stoichiometries of the dark binding of various psoralens to DNA have been investigated (Dall'Acqua et al., 1978; Isaacs et al., 1982).

A major obstacle to derive intercalation geometries from NMR spectra [for reviews, see Krugh & Nuss (1979) and Patel (1979)] arises from the uncertainty of fast signal averaging involving multiple binding modes (Reuben et al., 1978). We present an NMR line-width analysis in terms of exchange broadening that can be used as a criterion to exclude fast site averaging. Subsequently, drug overlap geometries are derived from the intercalation shifts and discussed in relation to the stereochemistry of the photoadducts of MOP and DNA.

Materials and Methods

Samples. 8-Methoxypsoralen (MOP) and d(pApT)$_4$ were purchased from Sigma Chemie (GmbH München) and Collaborative Research, Inc. (Waltham, MA), respectively. Buffer conditions of the NMR samples in H_2O and D_2O were 10 mM sodium cacodylate, 1 mM EDTA, and 1.1 M NaCl, pH 6.8, if not stated otherwise. Oligonucleotide concentrations were determined from the UV absorbance at 262 nm in the coil state (70 °C, no salt added) with an extinction coefficient of 19 000 cm^{-1} M^{-1} (base pair).

Precipitation Difference Spectra. NMR spectra were accumulated on a Bruker WH-270 instrument in correlation or Fourier transform mode with water presaturation. Spectra were referenced downfield from DSS with the water signal as a secondary standard. Signal assignments for complexed MOP were transferred from free MOP (cf. Figures 1 and 2).[2] Thus, temperature-dependent spectra of MOP could be measured with one sample. Precipitation of MOP during spectra accumulation was used to obtain difference spectra

† This work was supported by a grant from the Deutsche Forschungsgemeinschaft.
‡ Present address: Signal Research Center, Des Plaines, IL 60016.

[1] Abbreviations: DSS, 3-(trimethylsilyl)propanesulfonic acid sodium salt; EDTA, ethylenediaminetetraacetic acid; NMR, nuclear magnetic resonance; ppm, parts per million; Me_4Si, tetramethylsilane; MOP, 8-methoxypsoralen; MSD, minimum standard deviation(s).

[2] At low temperatures, the MOP solutions were metastable, and MOP precipitated after some hours even in the presence of d(pApT)$_4$. MOP was redissolved by raising the temperature to 75 °C for more than 12 h.

0006-2960/85/0424-7450$01.50/0

showing the MOP resonances but largely eliminating the signals from excess oligonucleotide (cf. Figure 2). Although the chemical shifts of MOP were strongly influenced by d-(pApT)$_4$, they did not change during precipitation. Evidently, the excess of oligonucleotide was big enough to keep the free duplex concentration and hence the ratio of bound to free MOP effectively constant during MOP precipitation.

Evaluation of Binding Parameters. With excess oligonucleotide, we assumed a simple binding equilibrium with $n = 2 \pm 1$, independent and equivalent sites per d(pApT)$_4$ duplex and an intrinsic binding constant K_{ic} (cf. Results and Discussion):

$$p_b/p_f = K_{ic}C_f \quad (1)$$

$$C_f = (n/2)C_0[\text{d(pApT)}_4] - p_bC_0(\text{MOP}) \quad (2)$$

where p_b and p_f ($=1 - p_b$) are the fractions of bound and free MOP, respectively, C_f is the concentration of free binding sites, and C_0 (MOP) and C_0[d(pApT)$_4$] are the total concentrations of MOP and oligonucleotide duplex, respectively. The value of $n = 2 \pm 1$ was estimated from UV absorbance titrations of MOP with poly(dA-dT)·poly(dA-dT) at 2 mM NaCl (Dall'Acqua et al., 1978). A small correction for higher ionic strengths was applied according to the ionic strength dependence of the number of MOP sites on DNA (Dall'Acqua et al., 1978). For fast chemical exchange, p_b is determined by the chemical shifts of the MOP resonances S_0, S_∞, and S at zero, infinite, and experimental concentrations of oligonucleotide, respectively:

$$p_b = (S - S_0)/(S_\infty - S_0) \quad (3a)$$

$$p_f = (S - S_\infty)/(S_0 - S_\infty) \quad (3b)$$

A simple expression for S_∞ is obtained from the ratio of eq 1 applied to two experiments at concentrations of free binding sites C_{f1} and C_{f2} with chemical shifts S_1 and S_2, respectively:

$$S_\infty = \frac{S_1 - (C_{f2}/C_{f1})S_2}{1 - C_{f2}/C_{f1}} \quad (4)$$

S_∞ was determined iteratively from the data of Table I by assuming $p_b = 1$ as a starting value. Only two iteration steps were required for consistency and the limiting intercalation shift of H5 (MOP). $S_0 - S_\infty = 1.2 \pm 0.1$ ppm was only 20% higher than the highest directly measured value of 7.82 − 6.81 = 1.01 ppm. Variation of n ($1 - \infty$) changed the limiting intercalation shifts by less than 6%.

Intercalation Shift Calculations. The calculation of intercalation shifts [for reviews, see Krugh & Nuss (1979) and Patel (1979)] was performed in two independent steps:

(1) We calculated isoshielding curves of the shifts produced in the intercalation plane by the ring currents and the atomic magnetic anisotropies of the two nearest base pairs (Giessner-Prettre & Pullman, 1976) and by the ring currents of the two next nearest-neighbor base pairs (Kroon et al., 1974). The base pairs were arranged parallel to the intercalation plane at 3.4 and 6.8 Å below and above the drug. The base pair arrangements were derived from six typical intercalation site geometries from the literature (cf. Table III) [for reviews, see Sobell (1980) and Rich et al. (1980)] in which all purine and pyrimidine residues were replaced by adenine and thymine, respectively. More intercalation geometries with similar base pair overlaps have been published (Jain et al., 1977, 1979; Berman et al., 1978; Wang et al., 1979; Reddy et al., 1979), also including deoxydinucleotides (Wang et al., 1978). The base pair turn angle between the nearest- and next nearest-neighbor base pair was assumed to be 34°, implying 2° unwinding (Alden & Arnott, 1975).

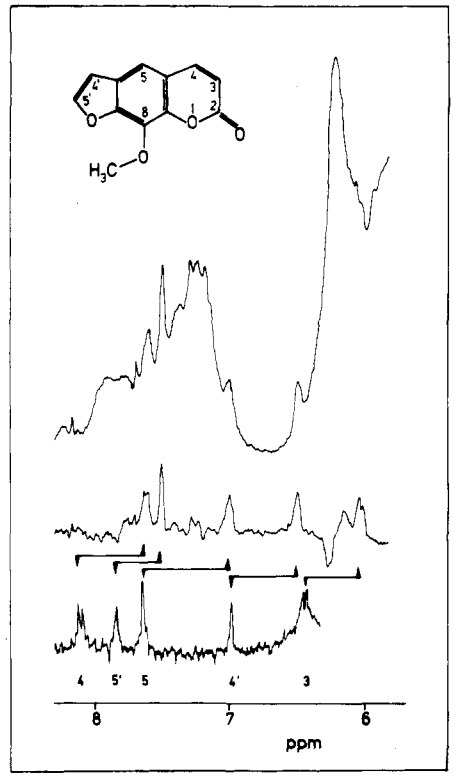

FIGURE 1: Intercalation shifts. ^{1}H NMR spectra of MOP in the absence (lower spectrum) and presence (middle spectrum) of 1.7 mM d(pApT)$_4$ at 17.3 °C in D_2O buffer. The latter curve represents a precipitation difference spectrum virtually eliminating the signals of excess d(pApT)$_4$. Spectra of freshly redissolved MOP (150 nmol in the 0.2-mL sample volume) in the presence of the oligonucleotide were accumulated overnight, allowing MOP to precipitate, and the difference of the first (top spectrum) and the last spectrum was calculated (middle spectrum).

(2) A scale model of MOP (Stemple & Watson, 1972) containing the measured intercalation shifts was systematically displaced on top of the calculated isoshielding curves in order to achieve a good fit between measured and calculated shifts. Deviations for the average methoxy signal were only included if the measured shift was outside the range defined by the two methyl positions rotated around the C8–O bond of MOP. Finally, we examined the best-fitting positions of the drug for steric strains from the sugar phosphate backbone (Miller et al., 1980). The separation of steps 1 and 2 is based on the concept of coplanar intercalation with the drug parallel to the adjacent base pairs and with the nucleotide conformation independent of the exact drug overlap. Evidently, the more realistic calculations in three dimensions (Ribas Prado & Giessner-Prettre, 1981) with simultaneous variation of nucleotide conformation and drug position are much more involved (Alden & Arnott, 1975; Berman et al., 1978). They might be warranted with additional information from the NMR signals of the nucleotides at the intercalation site.

RESULTS

Experimental Intercalation Shifts. The influence of d-(pApT)$_4$ on the ^{1}H NMR spectrum of MOP at 17.3 °C is demonstrated in Figure 1. The temperature dependence of the complexation shifts is presented in Figure 2. At high temperatures (>70 °C) where d(pApT)$_4$ is single stranded, it does not influence the MOP resonances. The continuous upfield shift of the MOP signals by d(pApT)$_4$ at lower temperatures indicates fast exchange between free and bound MOP. Below 10 °C, the complexation shifts start to level off at values between 0.3 and 0.9 ppm for the six MOP signals

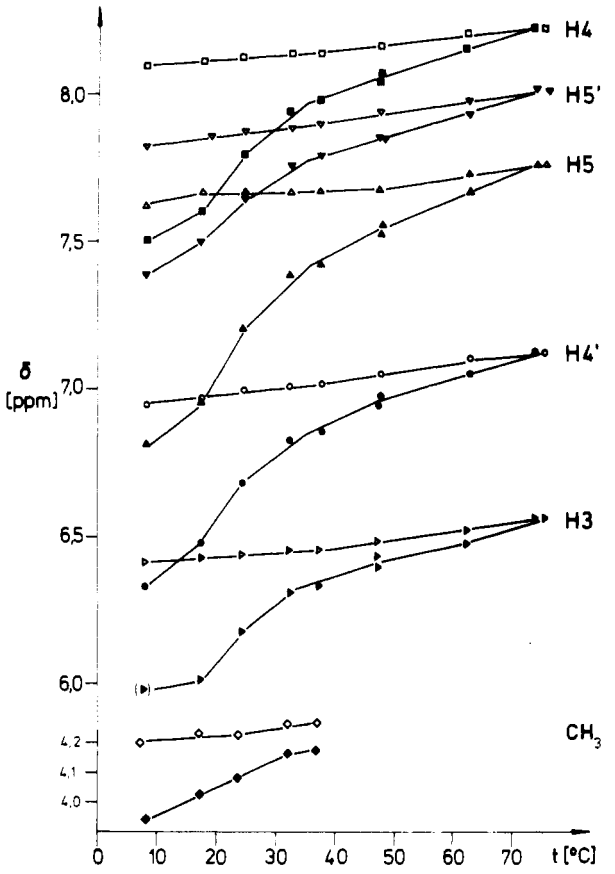

FIGURE 2: Temperature dependence of intercalation shifts. Chemical shifts of MOP protons in the absence (open symbols) and presence (closed symbols) of $d(pApT)_4$. Sample as in Figure 1.

Table I: Concentration Dependence of the H5 (MOP) Chemical Shift[a]

C_0 (mM)		
MOP	$d(pApT)_4$	chemical shift of H5 (ppm)
0.5		7.82
1.33	3.5	6.81
0.5	1.4	6.97

[a] Conditions: 45 mM sodium cacodylate, 38 mM potassium phosphate, 18 mM EDTA, and 950 mM NaCl, pH 6.3, 4 °C.

(Figure 2). The order of magnitude of these shifts suggests intercalation of MOP in the double-helical oligonucleotide (Krugh & Nuss, 1979).

The relative values of the complexation shifts of the six MOP signals are independent of temperature and degree of binding within ±10%. This finding suggests that the mode of binding remains the same in the observed temperature range between 4 and 32 °C: Either there is only one kind of binding site or, if there are several, they should be similar with respect to the relative intercalation shifts of the six MOP signals and/or their intercalation enthalpies.

The limiting intercalation shifts for completely bound MOP were obtained from the combined results of Figure 1 and additional spectra at higher concentrations and lower temperatures. From these spectra, the intercalation shift of the H5 (MOP) signal was determined (Table I). Its limiting value for complete binding was calculated as described under Materials and Methods, yielding a value of 1.2 ± 0.1 ppm. The chemical shifts of the remaining MOP protons could be measured most accurately at 17.3 and 7.3 °C with less excess oligonucleotide (Figure 1). To account for incomplete binding under these conditions, the complexation shifts of all MOP protons were multiplied by the ratio between the limiting and actual intercalation shifts of H5 (MOP). The average values of the limiting intercalation shifts obtained in this way at 7.3 and 17.3 °C are presented in Table II.

Table II: Limiting Values of Intercalation Shifts (ppm)

H3	H4	H5	CH_3	H4′	H5′	H (MOP)
0.73	0.88	1.20	0.36	0.90	0.63	shift

The distribution of the limiting intercalation shifts in the plane of the MOP molecule is represented in Figure 5. From their maximum at H5, the values continuously decrease toward H3 and H5′ close to the ends of the long axis (for numbering, cf. Figure 1). This is in contrast to the intercalation shifts reported for proflavin in poly(dA-dT) (Patel, 1977), 9-aminoacridine in d(ATGCAT) (Reuben et al., 1978), and ethidium bromide in CpG (Lee & Tinoco, 1978). With these dyes, an increase of the intercalation shifts was observed from the center toward the ends of the long axis. This qualitative difference of experimental intercalation shifts is the basis for the novel asymmetrical intercalation geometry of MOP in $d(pApT)_4$ suggested under Discussion.

Other Shift Mechanisms. The absence of some nonintercalation contributions to the observed complexation shifts was checked by considering solvent shifts, MOP aggregation shifts, and shifts by paramagnetic impurities. The chemical shifts and line widths of our samples were independent of EDTA concentration, e.g., 5 mM instead of 19 mM in the experiments summarized in Table I. The difference of the chemical shifts of the MOP protons in D_2O (DSS standard) and dimethyl sulfoxide (Me_4Si standard) was 0.04 ± 0.1 ppm, including the two major deviations at the methyl and H5′ protons. Tenfold dilution of MOP in aqueous solution changed its chemical shifts by less than 2% of the intercalation shifts. Shift contributions not included in the isoshielding curves used in our calculations (Giessner Prettre & Pullman, 1976) are usually smaller than 0.1 ppm (Krugh & Nuss, 1979).

Hydrogen-Bonded Protons of $d(pApT)_4$. In order to confirm the double-helical conformation of the oligonucleotide under our experimental conditions, we recorded its low-field spectrum in H_2O, where the signals of the exchangeable hydrogen-bonded protons from Watson–Crick base pairs can be detected. The spectrum contains a single broad signal at 13.35 ppm corresponding to one exchangeable proton per possible Watson–Crick base pair of the assumed oligonucleotide duplex. The chemical shift and the line width are very similar to the resonance previously assigned to the hydrogen-bonded imino protons of double-helical $d(pApT)_4$ at higher oligonucleotide concentrations (25 mg/mL, 0 °C, pH 7 in 0.1 M NaCl) (Patel & Tonelli, 1974). Between 12 and 27 °C, the signal disappears, as reported in the same paper. The spectrum and its disappearance at elevated temperatures demonstrate that at low temperatures $d(pApT)_4$ is basically double helical even at the reduced concentrations of our samples.

Exchange Broadening. The signals of the MOP protons are considerably broadened by the presence of $d(pApT)_4$ (Figure 1). The continuous shifts of the MOP signals upon addition $d(pApT)_4$ imply fast exchange between free and bound MOP. If the broadenings are also due to fast exchange, their values for the different MOP protons should be proportional to the squares of the intercalation shifts (eq 6). A corresponding plot is presented in Figure 3. It is linear with a correlation coefficient of 0.96.

The methoxy protons were not included in the plot. Their broadening upon binding is about 1.2 Hz too large with respect to the straight line in Figure 3. This is probably due to some

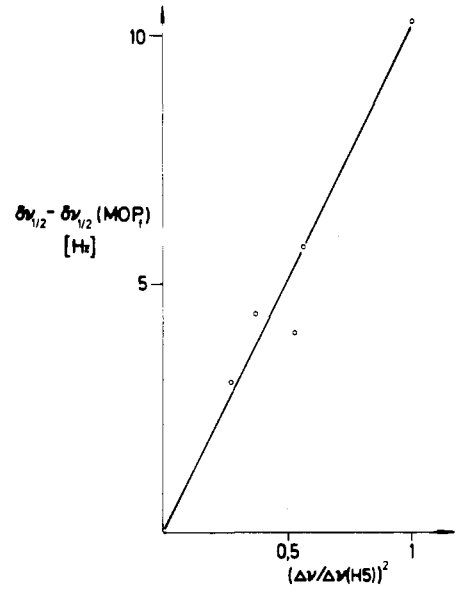

FIGURE 3: Exchange broadening of MOP signals. Difference of the NMR line widths of the MOP ring protons in the presence ($\delta\nu_{1/2}$) and absence [$\delta\nu_{1/2}$ (MOP_f)] of d(pApT)$_4$ at 17 °C (cf. Figure 1) vs. the square of the limiting intercalation shifts ($\Delta\nu$). $\Delta\nu$ (H5), maximum value of the limiting intercalation shifts (cf. Table II) used as a constant scaling factor.

freezing of internal rotation upon binding. Internal rotation of the methoxy protons in free MOP is indicated by the line widths. The ratio of the line width to $\sum_b r_{ab}^{-6}$ is much smaller for the methyl signals than for all other resonances (r_{ab} represents the distances to the neighboring protons (Stemple & Watson, 1972)]. For dipolar broadening and fast reorientation, the ratio is proportional to the correlation time of the magnetic nuclei.

We also tried alternative correlations for the MOP line widths expected for increased dipolar broadening by reduced molecular motions. The correlation coefficients of linear plots vs. $\sum_b r_{ab}^{-6}$ or vs. the intrinsic line widths of free MOP were only 0.25 and 0.73, respectively, even when admitting large intercepts (76% and 39% of average broadening, respectively, and excluding the methoxy protons. Evidently, fast chemical exchange gives a much better correlation than increased dipolar broadening.

Three-State Model of Exchange Broadening. With fast chemical exchange between free and bound MOP, we also considered the possibility of fast averaging of different chemical shifts of each MOP proton in multiple binding environments. The concomitant ambiguities for the geometrical interpretation of intercalation shifts have been discussed in the literature (Reuben et al., 1978).

The most obvious way to generate multiple binding modes would be by rotating the MOP molecule around its short pseudosymmetry axis, C5–C8. The strongest possible change in environment and chemical shift upon the rotation would be expected for the peripheral H3 and H5′ protons with no change at H5 on the axis. Consequently, the broadening of the MOP signals by fast exchange between the rotated binding modes would be negligible at H5 and increase toward the ends of the molecule in proportion with the square of the chemical shift differences between the two modes. This is in contrast to the observed line widths with a maximum value at H5. The broadening by the pseudosymmetrical rotation, if any, has to be small as compared to the broadening by fast averaging between the free and average bound states. This means that the rotation, if any, does not produce large chemical shift differences at the six monitored MOP protons.

For a quantitative consideration, we adopt the published expression for line broadening by fast exchange between more than two states with different chemical shifts values and equal intrinsic spin–spin relaxation times, T_2 (Piette & Anderson, 1959):

$$\pi\delta\nu_{1/2}^{ex} = \pi\delta\nu_{1/2} - T_2^{-1} = \frac{\tau T_2}{T_2 + \tau}\left[\sum_i p_i\omega_i^2 - \left(\sum_i p_i\omega_i\right)^2\right] \quad (5)$$

p_i is the fraction of all molecules in the ith state, and τ is the mean lifetime, i.e., the reciprocally averaged time between reorientations or collisions, which might bring about the change between the different states. We are interested in the case of three states with subscripts f, b, and b′ and express the Larmor frequencies (ω_i) by their differences between the free and the average of the two bound states (Δ) and between the two bound states (Δ):

$$\pi\delta\nu_{1/2}^{ex} = \frac{T_2\tau}{T_2 + \tau}(p_b + p_{b'})p_f\left[\Delta^2 + \frac{1}{p_f}\frac{p_b p_{b'}}{(p_b + p_{b'})^2}\Delta'^2\right] \quad (6)$$

At 17 °C (Figure 3), a value of $p_f = 0.41$ is obtained from eq 3, Figure 2, and Table II. Assuming furthermore $p_b = p_{b'}$ and $\Delta = \Delta'$, the broadening by Δ' should be 60% of the broadening by Δ'. Since with a pseudosymmetric rotation $\Delta' = 0$ for H5 and $\Delta' = \Delta$ at the other protons, 60% deviations from linearity should be observed in Figure 3. The actual deviations set a limit of $\Delta' \lesssim 0.5\Delta$. Accurate line-width measurements at lower fractions of free MOP could yield more stringent limits for Δ'/Δ (eq 6).

Intercalation Kinetics. The dissociation rate constant for intercalation was calculated from the exchange broadening on the basis of a simple one-step mechanism of intercalation. For two states, $p_{b'} = 0$ and $\tau \ll T_2$:

$$\tau^{-1} = \tau_f^{-1} + \tau_b^{-1} = k_R C_f + k_D \quad (7)$$

where k_R and k_D are the association and dissociation rate constants for intercalation and C_f is the concentration of free sites (Piette & Anderson, 1959). Equation 6 was solved for τ^{-1}:

$$\tau^{-1} = (\Delta[H5])^2 p_f p_b[\pi\delta\nu_{1/2}^{ex}/(\Delta_x/\Delta[H5])^2]^{-1} \quad (8)$$

and eq 7 for k_D (cf. eq 1)

$$k_D = \tau^{-1} p_f \quad (9)$$

The results for k_D are presented in the Arrhenius plot of Figure 4. The activation enthalpy is $\Delta H_D^* = 18$ kcal/mol. Comparable values have been reported for the dissociatin of ethidium bromide from DNA (18.5 kcal/mol) Bresloff & Crothers, 1975) and for the conversion of intercalated to outside-bound proflavin (14 and 17 kcal/mol for calf thymus and T_2 DNA, respectively) (Li & Crothers, 1969). The conversion is rate limiting for the complete dissociation process of proflavin at high ionic strengths. Consequently, it determines the overall activation enthalpy of dissociation under those salt conditions, which are similar to the ones applied in our study.

We estimate k_R from k_D and K_{ic}:

$$k_R = k_D K_{ic} \quad (10)$$

For nK_{ic}, a value of $(5.8 \pm 0.5) \times 10^3$ M^{-1} can be calculated from the data of Tables I and II and Figure 2 by use of eq 1, 2, and 3. This is in the same range as previously reported for MOP and poly(dA-dT) at lower ionic strengths (Dall'-Acqua et al., 1978). Assuming $n = 2$ (cf. Materials and Methods) yields $K_{ic} = 2.9 \times 10^3$ M^{-1}, and with $k_D = 7.5 \times$

Table III: Intercalation Shifts and Drug–Base Overlap Geometry[a]

intercalation site conformation	intercalator	oligonucleotide	ref	min SD (ppm) for symmetrical intercalation: parallel to base pairs, CH_3 (MOP) in major groove	parallel to base pairs, CH_3 (MOP) in minor groove	perpendicular to base pairs, furan (MOP) in major groove	perpendicular to base pairs, furan (MOP) in minor groove
1	proflavin	$d(pGpC)_3$	Alden & Arnott (1975)	0.48 (0.53)	0.70 (0.49)	0.41 (0.49)	0.48 (0.50)
2	ethidium	r-iodo-UpA	Tsai et al. (1977)	0.44 (0.71)	0.52 (0.64)	0.46 (0.48)	0.48 (0.51)
3	9-aminoacridine	r-iodo-CpG	Sakore et al. (1979)	0.50 (0.30)	0.61 (0.47)	0.52 (0.49)	0.56 (0.50)
4		rCpG	Berman et al. (1978)	0.64 (0.40)	0.59 (0.52)	0.54 (0.59)	0.46 (0.59)
5	proflavin	rCpG	Neidle et al. (1977)	0.53 (0.24)	0.48 (0.35)	0.44 (0.37)	0.40 (0.56)
6	proflavin	r-iodo-CpG	Reddy et al. (1979)	0.47 (0.29)	0.43 (0.47)	0.53 (0.58)	0.44 (0.69)
7	acridine orange	r-iodo-CpG	Reddy et al. (1979)	0.28 (0.41)	0.32 (0.57)	0.48 (0.48)	0.49 (0.53)

[a] Values in parentheses are purine and pyrimidine bases of published conformations exchanged. Conformations 1–4, "normal" symmetrical intercalation without hydrogen bounding to the drug; conformations 5 and 6, symmetrical intercalation in the presence of hydrogen bonds to the drug; conformation 7, asymmetrical intercalation; conformations 1 and 4, model calculations; conformations 2, 3, 5, 6, and 7, X-ray analysis of cocrystals of drugs and dinucleotides. For references to other published intercalation site geometries, cf. Materials and Methods.

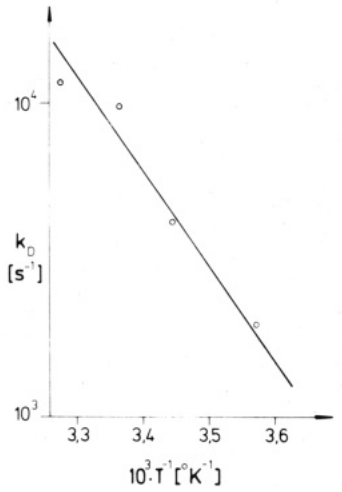

FIGURE 4: Arrhenius plot of the overall dissociation rate constant of the MOP–$d(pApT)_4$ intercalation complex (cf. eq 8 and 9).

10^2 s^{-1} (Figure 4), we obtain $k_R = 2 \times 10^6$ M^{-1} s^{-1}. Similar values have been reported for the binding of various acridines and phenacridines to DNA by the faster of the two observed intercalation modes (Wakelin & Waring, 1980).

Calculated Intercalation Shifts. The drug–base overlap in the intercalation complex was investigated by comparing the experimental intercalation shifts to calculated ring current and atomic magnetic anisotropy shifts.

Some typical results of the calculations are represented in Figure 5 together with the experimental intercalation shifts on a scale model of MOP. From the distribution of experimental and calculated shifts, we may derive some general conclusioins about the possible planar intercalation geometries of MOP. The maxima of the calculated shifts should be close to the center of MOP or at least between H8 and O–CH_3 and between H3 and H5′. This means that MOP has to be well sandwiched in between the bases rather than shifted far out of the range of base overlap.

Planar symmetrical intercalation with MOP parallel to the neighboring base pairs has been proposed in the literature as intermediate for photo-cross-link formation (cf. Discussion). The measured complexation shifts of MOP are also almost symmetrical around the short pseudosymmetry axis C8–C5. The minimum standard deviations (MSD) between calculated and measured shifts for various base pair geometries are represented in Table III. For the normal symmetrical intercalation geometries in the absence of hydrogen bonding to the intercalator (1–4 in Table III), the smallest value of MSD was 0.44 ppm. Including the base pair geometries in the presence of hydrogen bonding (5 and 6 in Table III) or

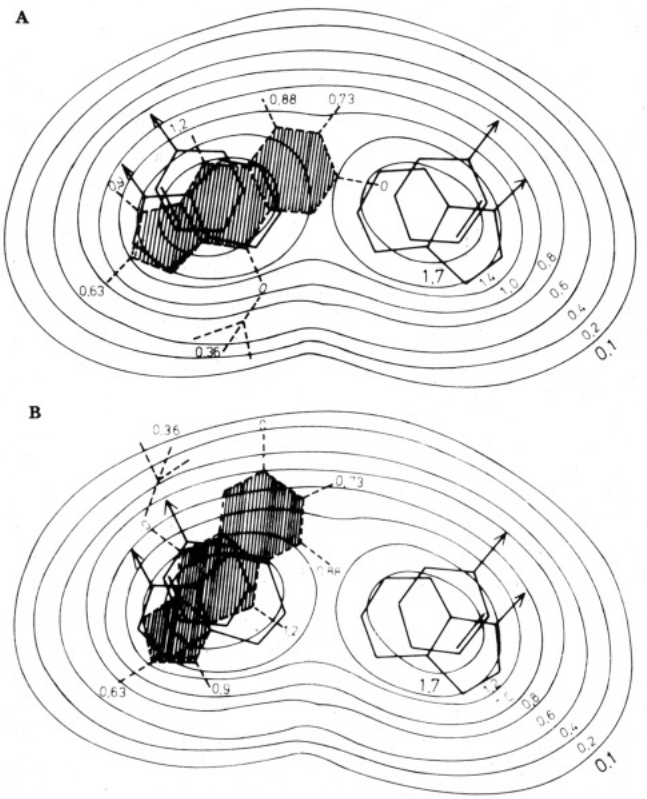

FIGURE 5: Asymmetrical MOP–base overlap. Calculated isoshielding curves (0.1–1.7 ppm) in the intercalation plane with base pair arrangement derived from Alden & Arnott (1975) (cf. conformation 1 of Table III). Measured complexation shifts (0.36–1.2 ppm) indicated on the scale model of MOP. Best fits obtained with the MOP methoxy group in the major (A) (standard deviation 0.11 ppm) and minor (B) (standard deviation 0.17 ppm) DNA grooves.

asymmetrical intercalation (7, Table III) reduces the smallest MSD somewhat to 0.28 ppm. Retaining the backbone geometries but exchanging purines and pyrimidines, i.e., converting from an A-T to a T-A sequence at the intercalation site, does not much reduce the minimum MSD, 0.24 and 0.25 ppm with base pair geometry 5 (Table III) and CH_3 (MOP) in the large and small grooves, respectively.

We also tried base–drug overlap geometries with MOP and the base pairs perpendicular. With the center of MOP on the short axis of the intercalation site, the smallest value of MSD was 0.35 ppm. This result applies to all base pair geometries including A to T exchanges (Table III).

Asymmetrical intercalation provides a considerable improvement of the fit between measured and calculated complexation shifts. Standard deviations are typically reduced to

less than half their minimum values for symmetrical intercalation, e.g., 0.11 ppm with base pair geometry 1 and CH_3 (MOP) in the large groove (Figure 5A). With CH_3 (MOP) in the small groove, a standard deviation of 0.17 ppm was obtained (Figure 5B). The position of MOP corresponding to the smallest standard deviations obtained in A-T and T-A environments is similar.

Discussion

Limit for Fast Site Averaging. Different modes of intercalation of various drugs in DNA have been reported on the basis of kinetic measurements (Bresloff & Crothers, 1975; Wakelin & Waring, 1980). In addition, symmetrical drugs always can form two indistinguishable symmetry-related complexes. In those two complexes, the environment of any individual MOP proton may be different if the intercalation is not symmetrical and the binding site does not have the same symmetry as the intercalator (Reuben et al., 1978). In NMR spectra, the signals of free and bound drug are usually averaged by fast chemical exchange [for a review; see Krugh & Nuss (1979)]. Consequently, we also considered average signals of the same proton in different environments produced by various modes of binding. The uncertainty introduced by fast signal averaging represents a major obstacle to derive structural information from NMR intercalation shifts, especially of symmetrical drugs (Reuben et al., 1978). Even though MOP is not symmetrical, the almost symmetrical distribution of intercalation shifts with respect to the short axis might suggest symmetrical averaging.

In this paper, we establish a limit for the effects of fast site averaging of MOP in $d(pApT)_4$. The method is based on the observed exchange broadenings of the various MOP resonances which are not compatible with the exchange between the quasi-symmetry-related intercalation modes but agree well with the exchange between free and bound drug.

Generally, the method should be applicable to other forms of multiple binding modes as the corresponding chemical shift differences (Δ') for the various drug protons do not vary in proportion to the average complexation shifts (Δ). As expected, small ratios of free to bound drug are desirable to detect small contributions by Δ' (eq 6).

The homogeneity of the binding sites for MOP on $d(pApT)_4$ is also indicated by the independence of the relative intercalation shifts on temperature.

Drug–Base Overlap Geometry. As explained above, the quasi-symmetrical distribution of the measured intercalation shifts on the MOP molecules is not due to fast quasi-symmetrical site averaging. At first glance, one therefore might attribute it to symmetrical intercalation. Closer inspection of the observed and calculated intercalation shifts, however, reveals that coplanar, symmetrical intercalation with the short axis of MOP either parallel or perpendicular to the 2-fold symmetry axis of the intercalation site does not produce a good fit.

Asymmetrical intercalation provides considerably better agreement. We cannot, however, strictly rule out symmetrical intercalation because of the uncertainty of the chemical shift calculations particularly with respect to the intercalation site geometry (cf. Materials and Methods). The original model of coplanar symmetrical intercalation between base pairs (Lerman, 1961) has been confirmed by a variety of solution and crystal studies [for reviews, see Neidle (1979), Sobell (1980), and Rich (1980)]. Asymmetrical intercalation was reported for cocrystals of dinucleotides and 9-aminoacridine (Sakore et al., 1979) or acridine orange (Reddy et al., 1979; Wang et al., 1979).

Photoreaction Intermediates. Both in the symmetrical and in the asymmetrical drug–base overlap geometries with the smallest deviations between measured and calculated complexation shifts, the MOP methoxy group is positioned in the large groove of the $d(pApT)_4$ double helix (Table III, Figure 5). This is in contrast to hypothetical models for the dark complex of psoralens and DNA, in which the methoxy group points to the small groove. These models were designed by approximating the geometry of photoadducts of MOP with thymidine in DNA. They were used as intermediates to explain photo-cross-link formation (Cole, 1970; Dall'Acqua et al., 1971) or the cis–syn[3] stereochemistry (Straub et al., 1981) observed for all isolated photoadducts of various psoralens and DNA (Kanne et al., 1982a,b; Peckler et al., 1982).

Our results suggest but do not prove that the base overlap of MOP in its equilibrium dark complex might not be favorable for the formation of the cis–syn photoadducts with thymidine in DNA. For pure geometrical proximity reasons, it would seem much better positioned for the formation of a cis–anti adduct. Other factors might determine the selection of the actually isolated cis–syn adducts, and large rotations of the drug from the equilibrium intercalation position might be involved.

This does not mean that the stereoselectivity cannot be strongly influenced by the dark complex with DNA as proposed previously (Straub et al., 1981). However, the selectivity might be due to the properties of some intercalated transition state instead of the equilibrium intercalation complex. For example, a reactive intermediate involving intercalation or even simple stacking with nucleotides based (Land et al., 1982) will always favor the cis over the trans conformations. Similarly, the intercalated transition states with the reactive bonds aligned as in the cis–syn or cis–anti adducts can be discriminated by different amounts of stacking or steric constraints. For example, in the intercalation site geometries 1 and 2 of Table III, the cis–syn adducts are consideraby favored by strong transition-state stacking. For other intercalation site conformations (e.g., 5 and 6 of Table III), the opposite preference can be derived.

Unfavorable prepositioning in the dark complex might introduce some additional activation barrier for the photoreaction. However, it does not exclude the strong influence of the conformation of the intercalation site on the stereoselectivity of the photoadducts of psoralens and DNA.

Acknowledgments

We thank G. Maass and E.-G. Niemann, who initiated this study, for continuous support and encouragement. The technical assistance of M. Fiedler is gratefully acknowledged.

Registry No. 8-MOP, 298-81-7; $d(pApT)_4$, 54690-94-7.

References

Alden, C. J., & Arnott, S. (1975) *Nucleic Acids Res. 2*, 1701–1717.

Berman, H. M., Neidle, S., & Stodola, R. K. (1978) *Proc. Natl. Acad. Sci. U.S.A. 75*, 828–832.

Bresloff, J. L., & Crothers, D. M. (1975) *J. Mol. Biol. 95*, 103–123.

Cole, R. S. (1970) *Biochim. Biophys. Acta 217*, 30–39.

Dall'Acqua, F., Marciani, S., Ciavatta, L., & Rodighiero, G. (1971) *Z. Naturforsch., B: Anorg. Chem., Org. Chem.*,

[3] Syn is defined with O1′ (MOP) and N1 (T) or C2 (MOP) and N1 (T) at adjacent corners of the cyclobutane for the furan and pyrone adducts, respectively. Cis refers to the location of MOP and T with respect to the plane of the cyclobutane.

Biochem., Biophys., Biol. 26B, 561-569.
Dall'Acqua, F., Terbogevich, M., Mariciani, S., Vedaldi, D., & Recher, M. (1978) *Chem.-Biol. Interact. 21*, 103-115.
Giessner-Rettre, C., & Pullman, B. (1976) *Biochem. Biophys. Res. Commun. 70*, 578-581.
Hearst, J. E. (1981) *J. Invest. Dermatol. 77*, 39-44.
Isaacs, S. T., Chun, C., Hyde, J. E., Rapoport, H., & Hearst, J. E. (1982) in *Trends in Photobiology* (Helene, C., Charlier, M., Montenay-Garestier, T., & Laustriat, G., Eds.) Plenum Press, New York and London.
Jain, S. C., Tsai, C. C., & Sobell, H. M. (1977) *J. Mol. Biol. 114*, 317-331.
Jain, S. C., Bhandary, K. K., & Sobell, H. M. (1979) *J. Mol. Biol. 135*, 813-840.
Kanne, D., Straub, K., Rapoport, H., & Hearst, J. E. (1982a) *Biochemistry 21*, 861-871.
Kanne, D., Straub, K., Hearst, J. E., & Rapoport, H. (1982b) *J. Am. Chem. Soc. 104*, 6754-6764.
Kroon, P. H., Kreishman, G. P., Nelson, J. H., & Chan, S. I. (1974) *Biopolymers 13*, 2571-2592.
Krugh, T. R., & Nuss, M. E. (1979) in *Biological Applications of Magnetic Resonance* (Shulman, R. G., Ed.) Academic Press, New York.
Land, E. J., Rushton, F. A. P., Beddoes, R. L., Bruce, J. M., Cernik, R. J., Dawson, S. C., & Mills, O. S. (1982) *J. Chem. Soc., Chem. Commun. 1*, 22-23.
Lee, C.-H., & Tinoco, I. (1978) *Nature (London) 274*, 609-610.
Lerman, L. S. (1961) *J. Mol. Biol. 3*, 18-30.
Li, H. J., & Crothers, D. M. (1969) *J. Mol. Biol. 39*, 461-477.
Miller, K. J., Macrea, J., & Pycior, J. F. (1980) *Biopolymers 19*, 2067-2089.
Neidle, S. (1979) *Prog. Med. Chem. 16*, 151-221.
Neidle, S., Achari, H., Taylor, G. L., Berman, H. M., Carrell, H. L., Glusker, J. P., & Stallings, W. C. (1977) *Nature (London) 269*, 304-307.
Patel, D. J. (1979) *Acc. Chem. Res. 12*, 118.
Patel, D. J., & Tonelli, A. E. (1974) *Biopolymers 13*, 1943-1964.
Parrish, J. A. (1981) *J. Invest. Dermatol. 77*, 167-171.
Parsons, B. J. (1980) *Photochem. Photobiol. 32*, 813-821.
Peckler, S., Graves, B., Kanne, D., Rapoport, H., Hearst, J. E., & Kim, S.-H. (1982) *J. Mol. Biol. 162*, 157-172.
Piette, L. H., & Anderson, W. A. (1959) *J. Chem. Phys. 30*, 899-908.
Reddy, B. S., Seshadri, T. P., Sakore, T. D., & Sobell, H. M. (1979) *J. Mol. Biol. 135*, 787-812.
Reuben, J., Baker, B. M., & Kallenbach, N. R. (1978) *Biochemistry 17*, 2915-2919.
Ribas Prado, F., & Giessner-Prettre, C. (1981) *Theor. Chem. (N.Y.) 1*, 81-98.
Rich, A., Quigley, G. J., & Wang, H. H.-J. (1980) in *Nucleic Acid Geometry and Dynamics* (Sarma, R. H., Ed.) Pergamon Press, New York.
Sakore, T. D., Reddy, B. S., & Sobell, H. M. (1979) *J. Mol. Biol. 135*, 763-785.
Sobell, H. M. (1980) in *Nucleic Acid Geometry and Dynamics* (Sarma, R. H., Ed.) Pergamon Press, New York.
Song, P. S., & Tapley, K. J., Jr. (1979) *Photochem. Photobiol. 29*, 1177-1197.
Stemple, N. R., & Watson, W. H. (1972) *Acta Crystallogr., Sect. B: Struct. Crystallogr. Cryst. Chem. B28*, 2485-2489.
Straub, K., Kanne, D., Hearst, J. E., & Rapoport, H. (1981) *J. Am. Chem. Soc. 103*, 2347-2355.
Tsai, C. C., Jain, S. C., & Sobell, H. M. (1977) *J. Mol. Biol. 114*, 301-315.
Wakelin, L. P. G., & Waring, M. J. (1980) *J. Mol. Biol. 144*, 183-214.
Wang, H. M.-J., Nathans, J., van der Marel, G., van Boom, J. H., & Rich, A. (1978) *Nature (London) 276*, 471-474.
Wang, H. H.-J., Quigley, G. J., & Rich, A. (1979) *Nucleic Acids Res. 6*, 3879-3891.

Poly(d2NH$_2$A-dT): Two-Dimensional NMR Shows a B to A Conversion in High Salt

Babul Borah,[‡] Jack S. Cohen,*[,‡] Frank B. Howard,[§] and H. Todd Miles[§]

Clinical Pharmacology Branch, Division of Cancer Treatment, National Cancer Institute, and Laboratory of Molecular Biology, National Institute of Arthritis, Diabetes, and Digestive and Kidney Diseases, National Institutes of Health, Bethesda, Maryland 20205

Received May 13, 1985

ABSTRACT: Poly(d2NH$_2$A-dT) forms a structure in high salt that is clearly distinct from the B form present in low salt. Two-dimensional nuclear Overhauser effect (2D NOE) NMR spectra establish that the conformation of the high-salt form is not Z. Correlations of observed cross peaks in the 2D NOE spectra and estimated interproton distances of the common DNA conformations are consistent only with an A form or closely related structure. This interpretation is also consistent with the negative circular dichroic band observed in the high-salt form of poly(d2NH$_2$A-dT) and in A-form ribohomopolymer helices containing 2NH$_2$A.

The conformational equilibrium between B and Z DNA has been extensively studied, though reasons for the interconversion are still not well understood. Several studies suggest that the Z form may be biologically important, possibly through a control function [Klysik et al., 1981; Nordheim et al., 1981; Hamada et al., 1982; for a review, see Zimmerman (1982)]. The fact that (dG-dC)$_n$ undergoes the B to Z transition while (dA-dT)$_n$ does not suggests a possible role of the third hydrogen bond present in GC pairs. In assessing this possibility it is important to examine a base pair having this property but

[‡] National Cancer Institute.
[§] National Institute of Arthritis, Diabetes, and Digestive and Kidney Diseases.